Escape rate of metastable states in a driven NbN superconducting microwave resonator

Baleegh Abdo,[a] Eran Segev, Oleg Shtempluck, and Eyal Buks
Department of Electrical Engineering, Technion, Haifa 32000, Israel

(Received 8 November 2006; accepted 28 February 2007; published online 30 April 2007)

We study thermal instability and formation of local hot spots in a driven nonlinear NbN superconducting microwave resonator. White noise injected into the resonator results in transitions between the metastable states via a process consisting of two stages. In the first stage, the input noise entering the system induces fluctuations in the resonator mode. While in the second one, these mode fluctuations result in phase transitions of the hot spot due to induced temperature fluctuations. The associated noise-activated escape rate is calculated theoretically and measured also experimentally by means of driving the system into stochastic resonance. A comparison between theory and experiment yields a partial agreement. © *2007 American Institute of Physics*.
[DOI: 10.1063/1.2722241]

I. INTRODUCTION

The simple model of noise activated escape of a Brownian particle over a potential barrier succeeds to explain the basic behavior of a large number of metastable systems in nature.[1] Examples of such systems can be found in almost all major fields of science: physics, chemistry, biology, and even engineering.[2] For instance, it explains biochemical reactions in alternating current-driven protein,[3] the lifetime of zero-voltage state in Josephson junctions,[4,5] the magnetization reversal in nanomagnets,[6–8] noise-activated switching in micro-[9] and nanomechanical[10,11] oscillators, and photon-assisted tunneling in semiconductor hetrostructures.[12]

A well-known pioneering work on the subject is Krammer's in 1940. In his seminal paper,[13] he derived relatively simple expressions for the thermally induced escape rate in a one-dimensional asymmetric double-well potential. In general, these escape rate expressions take the form of $\Gamma = \Gamma_0 \exp(-U_b/k_B T)$, where U_b is the potential barrier height, k_B is the Boltzmann's constant, T is the temperature (where the limit $k_B T \ll U_b$ is assumed), and Γ_0 is a rate prefactor. Important extensions and refinements to this formula aimed either to include a wider range of damping regimes[14–16] or accommodate the solutions to other cases such as nonequilibrium systems, have been contributed by many authors over the years.[17–19] Examples of such nonequilibrium systems are metastable potentials modulated by deterministic forces,[20] e.g., the case of stochastic resonance,[21,22] or metastable systems subjected to nonwhite noise.[23,24] Moreover, efforts have been invested also in extending Krammer's rate theory to describe metastable systems in the quantum limit,[1,25,26] where escape is dominated by tunneling.

In the present article we study the escape rate of metastable states of thermally instable superconducting stripline resonators both theoretically and experimentally. In recent studies[27,28] we have experimentally demonstrated such instability in NbN superconducting resonators. The measured response of the system to a monochromatic excitation was accounted for by a theoretical model, which attributed the instability to a local hot spot in the resonator, switching between the superconducting and the normal phases. Nonlinearity, according to this model, results due to coupling between the equations of motion for both, the mode amplitude in the resonator and the temperature of the hot spot. The coupling mechanism is based on the dependence of both, the resonance frequency and the damping rate of the resonator on the stripline impedance, which in turn depends on the temperature of the hot spot. Moreover, we have employed this instability to demonstrate experimentally intermodulation gain,[29] stochastic resonance,[30] self-sustained modulation of a monochromatic drive,[31,32] period doubling bifurcation, and noise squeezing.[33]

In the case of thermally instable superconducting stripline resonators, the escape mechanism governing the lifetime of the metastable states differs in general from many of the examples mentioned earlier. In this case, the input noise induces escape in a two-stage process. The direct coupling between the input noise and the driven mode leads to fluctuations in the mode amplitude, which in turn, induce fluctuations in the heating power applied to the hot spot. Consequently, the fluctuating heating power, which is characterized by a finite correlation time, leads to temperature fluctuations. Escape occurs when the temperature approaches the critical value and a phase transition takes place in the hot spot.

The remainder of this article is organized as follows. In Sec. II the steady state solutions of the equation of motion for the resonator-mode are derived for the case of local heating instability. In Sec. III a perturbative approach is applied in order to include the effect of thermal fluctuations. In Sec. IV an escape rate expression characterizing the metastable states of the resonator is obtained. In Sec. V a brief explanation regarding stochastic resonance measurement is given. While in Secs. V A and V B, stochastic resonance measurement results are employed in order to extract some of the transition rate parameters characterizing the system. Finally, a brief summary concludes this article in Sec. VI.

[a]Electronic mail: baleegh@tx.technion.ac.il

II. STEADY STATE SOLUTIONS

Consider the case of a superconducting stripline microwave resonator weakly coupled to a feedline. Driving the resonator by a coherent tone $a_1^{\text{in}}=b^{\text{in}}e^{-i\omega_p t}$ injected into the feedline, excites a mode in the resonator with an amplitude $A=Be^{-i\omega_p t}$, where ω_p is the drive angular frequency, b^{in} is a constant complex amplitude proportional to the drive strength, and $B(t)$ is a complex mode amplitude which is assumed to vary slowly on the time scale of $1/\omega_p$.

A. Mode amplitude

In this approximation, the equation of motion for B reads[34]

$$\frac{dB}{dt}=[i(\omega_p-\omega_0)-\gamma]B-i\sqrt{2\gamma_1}b^{\text{in}}+c^{\text{in}}, \tag{1}$$

where ω_0 is the angular resonance frequency, $\gamma=\gamma_1+\gamma_2$, where γ_1 is the coupling factor between the resonator and the feedline and γ_2 is the damping rate of the mode. The term c^{in} represents an input noise with a random phase

$$\langle c^{\text{in}}\rangle=0, \tag{2}$$

and autocorrelation functions given by

$$\langle c^{\text{in}}(t)c^{\text{in}}(t')\rangle=\langle c^{\text{in}^*}(t)c^{\text{in}^*}(t')\rangle=0, \tag{3}$$

$$\langle c^{\text{in}}(t)c^{\text{in}^*}(t')\rangle=G\omega_0\delta(t-t'). \tag{4}$$

By further assuming a thermal equilibrium condition at temperature T_{eff} and a relatively high temperature case $k_BT_{\text{eff}}\gg\hbar\omega_0$, one has

$$G=\frac{\gamma}{\omega_0}\frac{k_BT_{\text{eff}}}{\hbar\omega_0}. \tag{5}$$

Rewriting Eq. (1) in terms of the dimensionless time $\tau=\omega_0 t$ and using the steady state solution

$$B_\infty=\frac{i\sqrt{2\gamma_1}b^{\text{in}}}{i(\omega_p-\omega_0)-\gamma}, \tag{6}$$

yields the following compact form:

$$\frac{db}{d\tau}+\lambda b=\frac{c^{\text{in}}}{\omega_0}, \tag{7}$$

where $b=B-B_\infty$ represents the difference between the mode amplitude variable and the steady state solution, while λ reads

$$\lambda=\frac{\gamma-i(\omega_p-\omega_0)}{\omega_0}. \tag{8}$$

By applying the methods of Gardiner and Collett introduced in Ref. 35, one can obtain the following input-output relation:

$$b^{\text{out}}=b^{\text{in}}-i\sqrt{2\gamma_1}B, \tag{9}$$

which relates the output signal $a_1^{\text{out}}=b^{\text{out}}e^{-i\omega_p t}$ reflected off the resonator to the input signal $a_1^{\text{in}}=b^{\text{in}}e^{-i\omega_p t}$ entering the system.

Thus, the reflection parameter r in steady state is in general given by

$$r=\frac{b^{\text{out}}}{b^{\text{in}}}=\frac{\gamma_2-\gamma_1-i(\omega_p-\omega_0)}{\gamma_2+\gamma_1-i(\omega_p-\omega_0)}, \tag{10}$$

which is obtained by substituting B_∞ of Eq. (6) in the input-output relation given by Eq. (9) and dividing by the input drive amplitude b^{in}.

B. Heat balance of local heating

Assuming that the resonator nonlinearity is dominated by a local hot spot in the stripline resonator, and that the hot spot area is sufficiently small in order to consider its temperature T to be homogeneous, the heat balance equation reads[36]

$$C\frac{\mathrm{dT}}{\mathrm{dt}}=Q-W, \tag{11}$$

where C is the thermal heat capacity of the hot spot, Q is the power heating up the hot spot given by $Q=\alpha Q_t$, where Q_t is the total power dissipated in the resonator given by $Q_t=\hbar\omega_0 2\gamma_2|B|^2$ and α is a positive coefficient $0\leq\alpha\leq1$, while $W=H(T-T_0)$ is the power of the heat transfer to the coolant, which is assumed to be at a constant temperature T_0, where H is the heat transfer coefficient to the substrate.

In terms of the dimensionless time τ and the dimensionless temperature given by

$$\Theta=\frac{T-T_0}{T_c-T_0}, \tag{12}$$

Equation (11) reads

$$\frac{d\Theta}{d\tau}+g(\Theta-\Theta_\infty)=0, \tag{13}$$

where the following quantities have been defined:

$$g=\frac{H}{C\omega_0}, \tag{14}$$

and

$$\Theta_\infty=\frac{2\hbar\alpha\gamma_2|B|^2}{gC(T_c-T_0)}. \tag{15}$$

Hence, the steady state solution of Eq. (13), reads

$$\Theta_{\infty 0}=\frac{2\hbar\alpha\gamma_2|B_\infty|^2}{gC(T_c-T_0)}. \tag{16}$$

Moreover, if one further assumes that the fluctuation of B around B_∞ is relatively small, one can rewrite Eq. (13) in the following form:

$$\frac{d\theta}{d\tau}+g\theta=f, \tag{17}$$

where

$$\theta=\Theta-\Theta_{\infty 0}, \tag{18}$$

and f reads

$$f = g\Theta_{\infty 0}\left[\frac{b}{B_\infty} + \left(\frac{b}{B_\infty}\right)^*\right], \tag{19}$$

where second order in b was neglected.

In general, when a hot spot is generated or alternatively diminished in the stripline, it affects the resonator parameters ω_0, γ_1, γ_2, and α and may induce as a result jumps in the resonance response curve. Moreover, as we have already shown in previous publications,[27,28] most of the nonlinear experimental results exhibited by our superconducting NbN resonators can be modeled to a very good extent by assuming a step function dependence of the resonator parameters ω_0, γ_1, γ_2, and α on the hot spot dimensionless temperature Θ,

$$\omega_0 = \begin{cases} \omega_{0s} & \Theta < 1 \\ \omega_{0n} & \Theta > 1 \end{cases}, \quad \gamma_1 = \begin{cases} \gamma_{1s} & \Theta < 1 \\ \gamma_{1n} & \Theta > 1 \end{cases}, \tag{20}$$

$$\gamma_2 = \begin{cases} \gamma_{2s} & \Theta < 1 \\ \gamma_{2n} & \Theta > 1 \end{cases}, \quad \alpha = \begin{cases} \alpha_s & \Theta < 1 \\ \alpha_n & \Theta > 1 \end{cases}. \tag{21}$$

In addition, we have shown that, in general, while disregarding noise, the coupled Eqs. (7) and (13) may have up to two different steady state solutions. A superconducting steady state (S) of the hot spot exists when $\Theta_{\infty 0} < 1$, or alternatively when $E = |B|^2 < E_s$, where $E_s = gC(T_c - T_0)/2\alpha_s\gamma_{2s}\hbar$. Similarly, a normal steady state (N) of the hot spot exists when $\Theta_{\infty 0} > 1$, or alternatively when $E > E_n$, where $E_n = gC(T_c - T_0)/2\alpha_n\gamma_{2n}\hbar$.

III. FLUCTUATIONS

In this section we assume a nonzero noise term $c^{\text{in}}(t)$ entering the resonator, thus giving rise to fluctuations around the steady state solution of the system.

A. Mode fluctuations

In this case the solution of Eq. (7) reads

$$b(\tau) = b(0)e^{-\lambda\tau} + \frac{1}{\omega_0}\int_0^\tau c^{\text{in}}(\tau')e^{\lambda(\tau'-\tau)}d\tau'. \tag{22}$$

For relatively long times $\gamma\tau/\omega_0 \gg 1$ one gets by using Eq. (2) a zero mean value of the mode fluctuation b,

$$\langle b(\tau)\rangle = 0, \tag{23}$$

whereas by using Eqs. (3) and (4), respectively, one obtains the following autocorrelation functions:

$$\langle b(\tau_1)b(\tau_2)\rangle = \langle b^*(\tau_1)b^*(\tau_2)\rangle = 0, \tag{24}$$

and

$$\langle b(\tau_1)b^*(\tau_2)\rangle = \frac{G\omega_0}{2\gamma}e^{-\lambda^*|\tau_2-\tau_1|}, \tag{25}$$

which implies that fluctuations in the heating power of the hot spot are characterized by a finite correlation time which is set by the resonator parameter λ.

B. Local heating fluctuations

Similarly, the solution of the heat balance Eq. (17) can be written as

$$\theta(\tau) = \langle\theta(\tau)\rangle + \Delta_\theta(\tau), \tag{26}$$

where

$$\langle\theta(\tau)\rangle = \theta(0)e^{-g\tau}, \tag{27}$$

is the mean value of θ variable and

$$\Delta_\theta(\tau) = \int_0^\tau f(\tau')e^{g(\tau'-\tau)}d\tau', \tag{28}$$

is the deviation from the mean value.

The variance of θ, which is denoted as $\langle\Delta_\theta^2(\tau)\rangle$, can be derived with the use of Eqs. (28), (19), and (25). In the case of small τ, namely the case when $g\tau \ll 1$ and $|\lambda|\tau \ll 1$, one has to lowest order in τ,

$$\langle\Delta_\theta^2(\tau)\rangle = \frac{g^2\Theta_{\infty 0}^2}{|B_\infty|^2}\frac{2G\omega_0\tau^2}{\gamma}. \tag{29}$$

On the other hand, for relatively long times $g\tau \gg 1$ one finds

$$\langle\Delta_\theta^2\rangle = \frac{G\Theta_{\infty 0}^2}{|B_\infty|^2}\frac{g\omega_0^2}{\gamma}\frac{\gamma + g\omega_0}{(\gamma + g\omega_0)^2 + (\omega_p - \omega_0)^2}. \tag{30}$$

As transitions between S and N states depend also on the rate at which the temperature of the hot spot changes, one needs to calculate the fluctuations in this quantity as well. Thus, by taking the square of Eq. (17) one obtains

$$\zeta^2 + g\frac{d(\theta^2)}{d\tau} + g^2\theta^2 = f^2, \tag{31}$$

where the variable ζ represents the temperature change rate

$$\zeta(\tau) \equiv \frac{d\theta}{d\tau}. \tag{32}$$

Expressing $\zeta(\tau)$ as a sum of a mean value and a deviation terms in a similar manner to Eq. (26) yields

$$\zeta(\tau) = \langle\zeta(\tau)\rangle + \Delta_\zeta(\tau). \tag{33}$$

To evaluate the variance of $\zeta(\tau)$, which is denoted as $\langle\Delta_\zeta^2(\tau)\rangle$, in the limit of relatively long times we employ Eqs. (31), (30), and (19) and the autocorrelation functions given in Eqs. (24) and (25) to get

$$\langle\Delta_\zeta^2\rangle = \frac{g^2G\Theta_{\infty 0}^2}{|B_\infty|^2}\frac{\omega_0}{\gamma}\frac{(\omega_p - \omega_0)^2 + \gamma(\gamma + g\omega_0)}{(\gamma + g\omega_0)^2 + (\omega_p - \omega_0)^2}. \tag{34}$$

IV. ESCAPE RATE

Escape from S to N states originates from a flux at point $\Theta = 1$ (or $\theta = 1 - \Theta_{\infty 0}$) flowing from $\Theta < 1$ to $\Theta > 1$, or vise versa for the case of escape from N to S states. Thus, the escape rate is given by

$$\Gamma = \omega_0 \int_0^\infty \zeta f(1 - \Theta_{\infty 0}, \zeta) d\zeta, \tag{35}$$

where $f(\theta, \zeta)$ is the joint probability distribution function of the random variables θ and ζ. As was shown earlier, in the limit of relatively long times where $g\tau \gg 1$, the expectation values $\langle\theta\rangle$ and $\langle\zeta\rangle$ vanish. In general, $f(\theta, \zeta)$ is expected to represent a joint normal distribution. Moreover, θ and ζ variables become statistically independent as the expectation value $\langle\theta^2\rangle$ becomes time independent (which applies in the above limit $g\tau \gg 1$). This can be readily inferred from the following relation:

$$\langle \Delta_\theta \Delta_\zeta \rangle = \frac{1}{2} \frac{d\langle\theta^2\rangle}{d\tau} - \langle\theta\rangle\langle\zeta\rangle, \tag{36}$$

which can be obtained by a direct substitution of Δ_θ and Δ_ζ definitions given by Eqs. (26) and (33).

Thus, by applying the previous approximations one finds

$$\Gamma = \frac{\omega_0 \exp\left[-\frac{(1-\Theta_{\infty 0})^2}{2\langle\Delta_\theta^2\rangle}\right]}{2\pi\sqrt{\langle\Delta_\theta^2\rangle\langle\Delta_\zeta^2\rangle}} \int_0^\infty \zeta \exp\left(-\frac{\zeta^2}{2\langle\Delta_\zeta^2\rangle}\right) d\zeta. \tag{37}$$

Furthermore, by evaluating the above integral, substituting instead of G and $\Theta_{\infty 0}$ [given by Eqs. (5) and (16) respectively], and using the simplifying notations

$$C\prime = \frac{1}{2} \frac{(\gamma + g\omega_0)^2 + (\omega_p - \omega_0)^2}{g\omega_0(\gamma + g\omega_0)}, \tag{38}$$

$$\Gamma_0 = \frac{\omega_0}{2\pi} \sqrt{\frac{g[(\omega_p - \omega_0)^2 + \gamma(\gamma + g\omega_0)]}{\omega_0(\gamma + g\omega_0)}}, \tag{39}$$

one gets

$$\Gamma = \Gamma_0 \exp\left[-\frac{C\prime(U_c - U_\infty)^2}{U_\infty k_B T_{\text{eff}}}\right], \tag{40}$$

where

$$U_\infty = \hbar\omega_0 |B_\infty|^2, \tag{41}$$

is the energy stored in the resonator corresponding to the steady state amplitude B_∞, and

$$U_c = \hbar\omega_0 |B_c|^2, \tag{42}$$

is the mode energy corresponding to the critical amplitude B_c at which $\Theta_{\infty 0} = 1$, namely

$$1 = \Theta_{\infty 0} = \frac{2\hbar\alpha\gamma_2 |B_c|^2}{gC(T_c - T_0)}. \tag{43}$$

Note that typically in our NbN devices[28] $\gamma/g\omega_0 \simeq 10^{-2}$. Thus, by assuming the limit $\gamma/g\omega_0 \ll 1$, and the resonance case $\omega_p = \omega_0$, the above rate expression appearing in Eq. (40) reduces into

$$\Gamma = \frac{\sqrt{g\omega_0\gamma}}{2\pi} \exp\left[-\frac{1}{2}\frac{(U_c - U_\infty)^2}{U_\infty k_B T_{\text{eff}}}\right]. \tag{44}$$

V. STOCHASTIC RESONANCE

In order to examine experimentally the escape rate expression derived in Eq. (40), we employed stochastic resonance technique. Basically, stochastic resonance phenomenon demonstrates how a weak periodic signal, applied to a nonlinear metastable system, can be amplified at the system output with the aid of certain amount of zero-mean Gaussian white noise. The amplification of the signal occurs when a resonant cooperation is established between the small periodic signal and the white noise entering the system. In general, such a coherent interaction between the signal and the noise occurs when the angular frequency Ω of the signal, which periodically modulates the double-well potential of the system, becomes comparable to the escape rate of the metastable states in the presence of the white noise.

One advantage of applying this measurement technique is that once the system is tuned at the stochastic resonance condition statistical data belonging to both metastable transitions can be gathered simultaneously.

In the experiment we employed a superconducting resonator which is made of NbN and implements a stripline geometry. The center conductor film of the resonator of thickness 2200 Å was direct current-magnetron sputtered on a 34 mm × 30 mm × 1 mm sapphire substrate in an ambient gas mixture of Ar/N_2 at room temperature. The resonator patterning was done using standard ultraviolet lithography and ion milling. Additional fabrication process parameters are listed in Ref. 27. Whereas further modeling and characterization of these nonlinear devices are discussed in Ref. 28.

One direct manifestation of the metastability states of the resonator, is the occurrence of jumps in the resonance line shape as can be seen for example in Fig. 2(a), where a reflection parameter measurement of the first resonance mode of the resonator at $f_0 = \omega_0/2\pi \simeq 2.575$ GHz is shown. The different plots corresponding to an increasing input power were shifted downward by a constant offset for clarity. Moreover, as the pump frequency is swept in the forward and backward directions two frequency hysteresis loops emerge at both sides of the resonant curve. Thus revealing the frequency range at which the system is metastable.

On the other hand, in Fig. 2(b) we show a reflected power hysteretic behavior measured at a constant frequency $f_p = \omega_p/2\pi = 2.565$ GHz as the input power is swept up and down. This frequency was chosen as it falls within the instable region of the fundamental mode for a certain input power range as can be inferred from the measurements appearing in panel (a). Thus, in order to drive our resonators into metastability, we have applied based on the earlier observations a coherent microwave signal at frequency f_p and input power of $P_0 = -21.5$ dBm. Moreover, in order to tune the resonator into stochastic resonance condition, we have applied a small sinusoidal forcing to the system in the form of amplitude modulation (AM) and injected a thermal white noise with an adjustable intensity to the resonator port. The applied noise intensity was measured and calibrated separately using a spectrum analyzer.

A schematic illustration of the stochastic resonance measurement setup used is depicted in Fig. 1. A continuous mi-

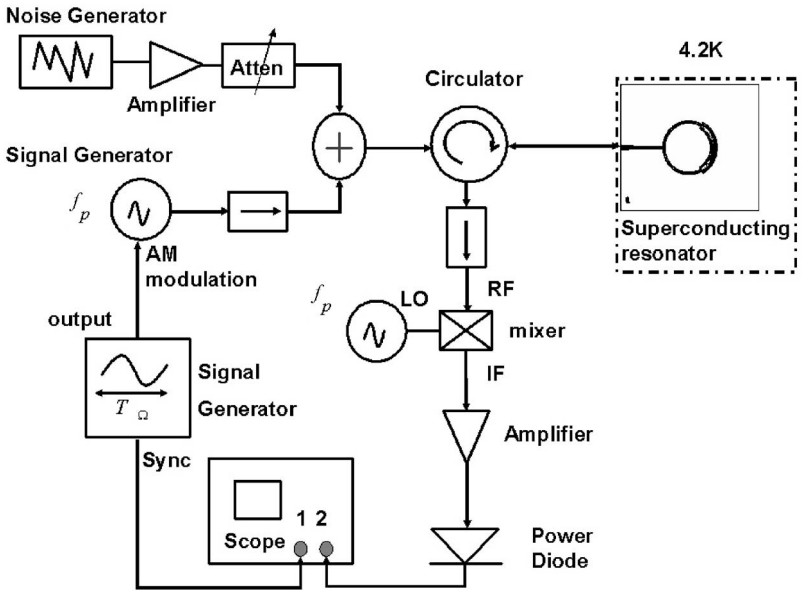

FIG. 1. Schematic block diagram of the experimental setup used. The microwave signal generator and the local oscillator at frequency f_p were phase locked. The layout of the resonator is shown at the top-right corner.

crowave signal at frequency f_p is amplitude modulated at frequency $f_\Omega = \Omega/2\pi = 1$ kHz. The modulated signal which effectively modulates the height of the potential barrier is combined with a white noise generated by a noise source and fed to the superconducting resonator. While the reflected signal off the resonator is mixed with a local oscillator phase-locked at frequency f_p and measured in the time domain using an oscilloscope. Additional information regarding stochastic resonance phenomenon measured in these nonlinear superconducting resonators is summarized in Ref. 30.

A. Escape rate measurement

At stochastic resonance condition, the lifetime of the metastable states becomes approximately equal to half the modulation period. Thus, assuming that the system has two metastable states designated by S_u and S_d (corresponding eventually to S and N states), it is expected to have one metastable state escape event each half time cycle. Such behavior is indeed seen in Fig. 3, which shows a typical result taken in the time domain at stochastic resonance condition, where the jumps appearing in the output signal correspond to alternating $S_d \rightarrow S_u$ and $S_u \rightarrow S_d$ transitions.

The blue dotted line in the figure represents the amplitude modulation signal, which modulates the escape rates Γ_1 and Γ_2 of the corresponding transitions $S_d \rightarrow S_u$ and $S_u \rightarrow S_d$, while the green solid line represents the modulated signal. In the vicinity of the minimum (maximum) points of the amplitude modulation signal (the blue dotted line), the escape rate $\Gamma_1(\Gamma_2)$ obtains its largest value, which is denoted as $\Gamma_{m1}(\Gamma_{m2})$. Hence, by letting $\tau_1(\tau_2)$ be the time difference between the time of the transition event $S_d \rightarrow S_u(S_u \rightarrow S_d)$ and the time at which the corresponding escape rate assumes its largest value, [namely the time at which Γ_1 equals Γ_{m1} (Γ_2 equals Γ_{m2})], the probability density characterizing this random variable $\tau_1(\tau_2)$ which will be denoted by $f_1(\tau_1)[f_2(\tau_2)]$, could be determined experimentally by building a normalized histogram of the measured times $\tau_1(\tau_2)$.

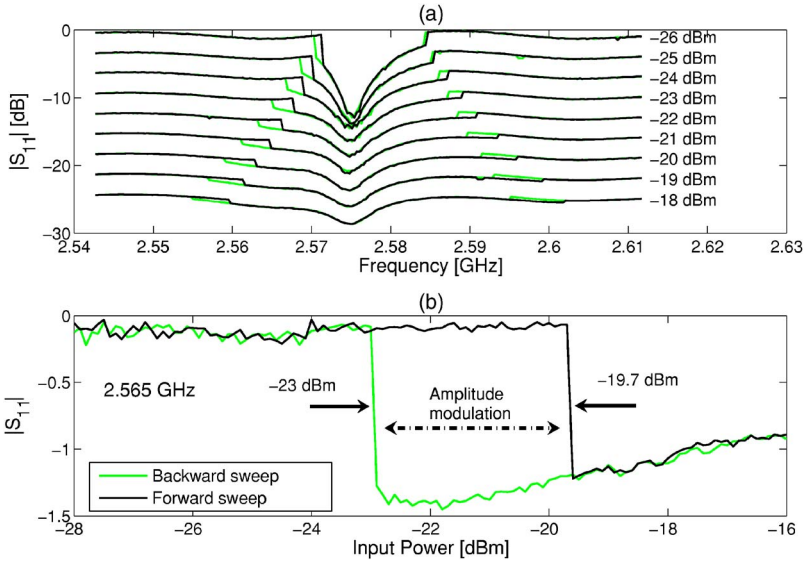

FIG. 2. (Color online). (a) Forward and backward frequency sweeps applied to the first mode of the resonator at ~2.575 GHz. The sweeps exhibit hysteresis loops at both sides of the resonance line shape. The plots corresponding to different input powers were shifted by a vertical offset for clarity. (b) Reflected power hysteresis measured at a constant angular frequency of $\omega_p = 2\pi 2.565$ GHz which resides within the left-side metastable region of the resonance. For both plots the black (dark) line represents a forward sweep whereas the green (light) line represents a backward sweep.

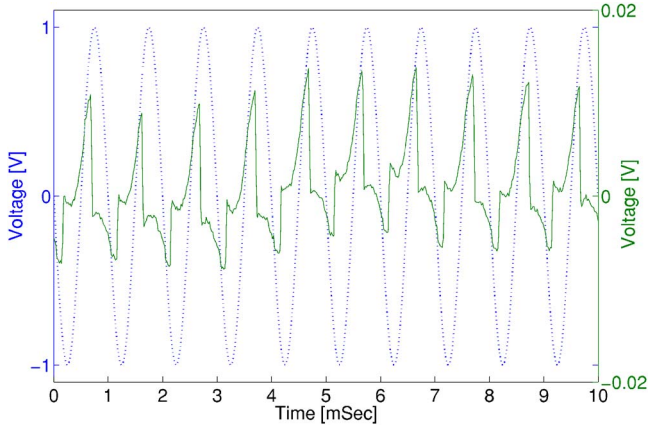

FIG. 3. (Color online). A typical snapshot of the time domain as the resonator is tuned into stochastic resonance condition. The solid (green) line represents the reflected modulated signal, corresponding to ten modulation cycles out of 5000 employed in the analysis. The dotted (blue) sinusoidal line represents the modulation signal applied to the microwave signal generator.

As can be seen from Eq. (A12) in the Appendix, the prefactors Γ_{m1} and Γ_{m2} can be estimated from the expectation value and the variance of the corresponding random variables τ_1 and τ_2. However, a more accurate value of the prefactor Γ_m can be obtained by invoking Eq. (A3) and employing a probability density function $f(\tau)$ fitted to the data.

In Figs. 4(a) and 4(b) we show the measured probability densities $f_1(\tau_1)$ and $f_2(\tau_2)$ extracted from 5000 modulation cycles sampled in the time domain. The solid line in both panels correspond to a Gaussian function fitted to the probability density measured in each case. The transition rate $\Gamma_1(\Gamma_2)$ as a function of the random variable $\tau_1(\tau_2)$, which is calculated using Eq. (A3) and the Gaussian fit applied to the data, is shown in the inset of Fig. 4(a) [Fig. 4(b)]. From these plots one can estimate the following rate values $\Gamma_{m1} \simeq 4.6 \times 10^5$ Hz and $\Gamma_{m2} \simeq 2.7 \times 10^5$ Hz which, as stated before, correspond to the transitions $S_d \rightarrow S_u$ and $S_u \rightarrow S_d$, respectively.

TABLE I. Calculated and measured model parameters.

	$S_d \rightarrow S_u$	$S_u \rightarrow S_d$
$g(10^{-3})$	1.56	1.56
γ(MHz)	37.6	18.6
P_c (dBm)	−23	−19.6
$\Delta P_{\text{in}}(10^{-6}$ W)	0.12	1.2
$\lvert r\rvert^2$	0.55	0.8
$k_B T_{\text{eff}}$(fW/Hz)	1.4	1.4
Γ_0(Hz)	8×10^6	8.3×10^6
Γ_m(Hz) (calc.)	7.8×10^6	1.9×10^6
Γ_m(Hz) (meas.)	4.6×10^5	2.7×10^5

B. Discussion

In order to obtain an estimate for the escape rates Γ_{m1} and Γ_{m2} corresponding to the $S_d \rightarrow S_u$ and $S_u \rightarrow S_d$ transitions, respectively, based on the theoretical model, we rewrite Eq. (40) in terms of the feedline input power P_{in} at the extremum of the AM, and the power difference $\Delta P_{\text{in}} \equiv P_c - P_{\text{in}}$, where P_c is the critical input power being proportional to the critical energy U_c,

$$\Gamma_m = \Gamma_0 \exp\left[-C\prime \left(\frac{\Delta P_{\text{in}}}{P_{\text{in}}} \right)^2 \frac{U_\infty}{k_B T_{\text{eff}}} \right]. \tag{45}$$

Furthermore, instead of the stored energy U_∞ appearing in the earlier expression, one can substitute the following equation:

$$U_\infty = \frac{P_{\text{in}}(1 - |r|^2)}{2\gamma}, \tag{46}$$

which basically relates the transmitted input power to the resonator $P_t = P_{\text{in}}(1 - |r|^2)$ in steady state, to the dissipated power at resonance which according to Eq. (1) is given by $2\gamma U_\infty$.

Estimates for the model parameters corresponding to both $S_d \rightarrow S_u$ and $S_u \rightarrow S_d$ transitions are summarized in Table I. Estimates for the coupling parameter γ corresponding to

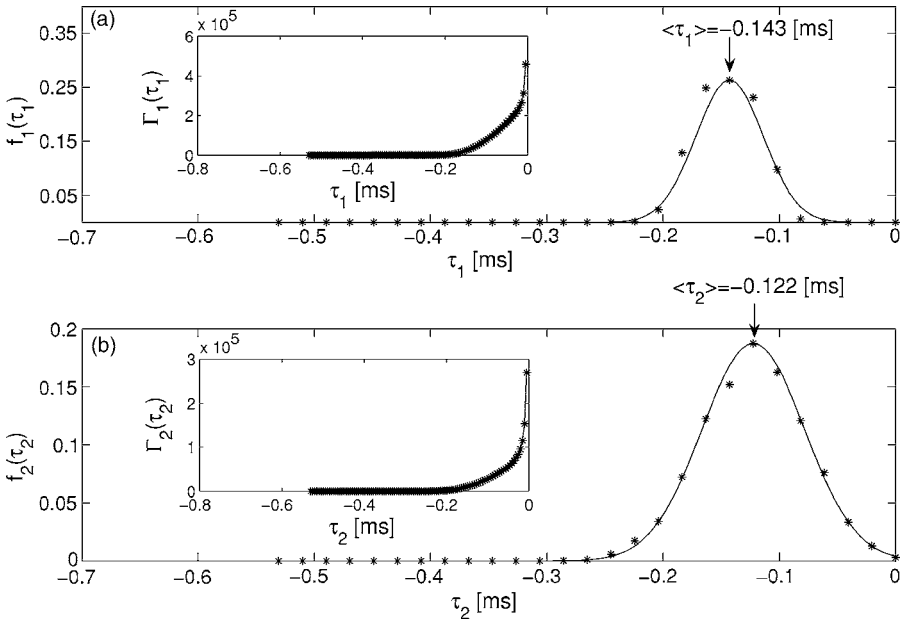

FIG. 4. Gaussian probability density functions $f_1(\tau_1)$ and $f_2(\tau_2)$ fitted to the experimental data which correspond to the $S_d \rightarrow S_u$ transition in panel (a) and to the $S_u \rightarrow S_d$ transition in panel (b). The escape rates Γ_1 and Γ_2 associated with both transitions are plotted in the insets of panels (a) and (b), respectively as a function of the random time variables τ_1 and τ_2 according to Eq. (A3).

the S_u and the S_d states have been extracted indirectly by fitting Eq. (10) to the measured reflection parameter curves versus the pump frequency ω_p in the vicinity of the resonance.[37] Whereas, the cooling parameter g, which is defined in Eq. (14), has been estimated using experimentally measured material properties of NbN,[38–40] yielding the value $g \simeq 1.56 \times 10^{-3}$ (see Refs. 28 and 32). Employing these estimates together with the experimental values of P_c, ΔP_{in}, and r and substituting in Eq. (45) yield a rough estimate for the escape rates $\Gamma_{m1} \simeq 7.8 \times 10^6$ Hz and $\Gamma_{m2} \simeq 1.9 \times 10^6$ Hz belonging to the $S_d \rightarrow S_u$ and the $S_u \rightarrow S_d$ transitions, respectively.

This discrepancy, found between the values of the escape rates obtained using the theoretical model as opposed to those extracted from the experimental data by about one order of magnitude, can be attributed to a large extent to the accumulated errors in the estimated values of the model parameters, some of which have been evaluated indirectly, as well as to many simplifying assumptions which the theoretical model employs in order to derive an analytical expression for the escape rate. As examples for model parameters which were determined indirectly and yet have a large effect on the escape rate value, one can name the g parameter which depends among others on the geometry of the hot spot and the thermal properties of the deposited NbN film, which are not known precisely, and also the coupling factor γ which is extracted using an approximate fitting procedure.[37]

VI. SUMMARY

In conclusion, a noise-activated escape rate expression was derived for the case of a nonlinear superconducting microwave resonator having a local-thermal instability. In order to determine the escape rate experimentally, stochastic resonance measurements were applied. A partial agreement is found between the theoretical and the experimental results up to one order of magnitude. Such discrepancy as has been argued, can be easily accounted for, by some of the shortcomings of the model and by possible uncertainties in the value of a few model parameters.

ACKNOWLEDGMENTS

This work was supported by the German Israel Foundation under Grant No. 1–2038.1114.07, the Israel Science Foundation under Grant No. 1380021, the Deborah Foundation, the Poznanski Foundation, and MAFAT.

APPENDIX: TRANSITION LIFETIME

Consider a system which has in general two metastable states designated by S_a and S_b and assume that at time $t=-t_0$ the system is in state S_b, where $t_0>0$. The transition rate Γ of the process $S_b \rightarrow S_a$ depends on an externally applied time varying parameter $p(t)$. Further assume that for p close to some fixed value p_m the transition rate is given approximately by

$$\Gamma(p) = \Gamma_m \exp\left(-\kappa^2 \frac{p-p_m}{p_m}\right), \tag{A1}$$

where both Γ_m and κ are positive constants.

The probability distribution function $F(\tau)$ for a transition of the kind $S_b \rightarrow S_a$ to take place within the time interval $(-t_0,\ \tau)$ is given by

$$F(\tau) = \int_{-t_0}^{\tau} f(t)dt, \tag{A2}$$

where $f(\tau)$ is the corresponding probability density. By definition, the following holds:

$$\frac{f(\tau)}{1-F(\tau)} = \Gamma[p(\tau)]. \tag{A3}$$

The initial condition $F(-t_0)=0$ and Eq. (A3) yield

$$f(\tau) = \Gamma[p(\tau)]\exp\{-\int_{-t_0}^{\tau} \Gamma[p(t)]dt\}. \tag{A4}$$

Further assume the case where at time $t=0$ the function $p(t)$ obtains a local minimum $p(0)=p_m$. Near $t=0$ one has

$$p(t) = p_m(1+\Omega^2 t^2) + O(t^3). \tag{A5}$$

Thus, in the vicinity of $t=0$ Eq. (A1) becomes

$$\Gamma(t) = \Gamma_m \exp(-\kappa^2\Omega^2 t^2), \tag{A6}$$

and the following holds:

$$f(\tau) = \Gamma_m \exp\left[-\kappa^2\Omega^2\tau^2 - \sqrt{\pi}\frac{\Gamma_m}{\kappa\Omega}\frac{\text{erf}(\kappa\Omega\tau)+\text{erf}(\kappa\Omega t_0)}{2}\right]. \tag{A7}$$

Keeping terms up to second order in $\kappa\Omega\tau$ and assuming the case where

$$\left(-\kappa\Omega t_0 + \frac{\Gamma_m}{2\kappa\Omega}\right)^2 \gg 1, \tag{A8}$$

allow approximating the probability density $f(\tau)$ by

$$f(\tau) = \frac{\Omega\kappa}{\sqrt{\pi}}\exp\left[-\kappa^2\Omega^2\left(\tau + \frac{\Gamma_m}{2\kappa^2\Omega^2}\right)^2\right]. \tag{A9}$$

In this approximation the random variable τ has a normal distribution function with a mean value

$$\mu_\tau = -\frac{\Gamma_m}{2\kappa^2\Omega^2}, \tag{A10}$$

and a variance

$$\sigma_\tau^2 = \frac{1}{2\kappa^2\Omega^2}, \tag{A11}$$

whereas, the parameters Γ_m and κ are given by

$$\Gamma_m = -\frac{\mu_\tau}{\sigma_\tau^2} \tag{A12}$$

and

$$\kappa^2 = \frac{1}{2\sigma_\tau^2 \Omega^2}. \tag{A13}$$

[1] P. Hänggi, P. Talkner, and M. Borkovec, Rev. Mod. Phys. **62**, 251 (1990).
[2] *Activated Barrier Crossing; Applications in Physics, Chemistry, and Biology*, edited by G. R. Fleming and P. Hänggi (World Scientific, Singapore, 1993).
[3] E. H. Serpersu and T. Y. Tsong, J. Membr. Biol. **74**, 191 (1983).
[4] T. A. Fulton and L. N. Dunkleberger, Phys. Rev. B **9**, 4760 (1974).
[5] M. Büttiker, E. P. Harris, and R. Landauer, Phys. Rev. B **28**, 1268 (1983).
[6] W. Wernsdorfer, E. B. Orozco, K. Hasselbach, A. Benoit, B. Barbara, N. Demoncy, and A. Loiseau, Phys. Rev. Lett. **78**, 1791 (1997).
[7] R. H. Koch, G. Grinstein, G. A. Keefe, Y. Lu, P. L. Trouilloud, W. J. Gallagher, and S. S. P. Parkin, Phys. Rev. Lett. **84**, 5419 (2000).
[8] E. B. Myers, F. J. Albert, J. C. Sankey, E. Bonet, R. A. Buhrman, and D. C. Ralph, Phys. Rev. Lett. **89**, 196801 (2002).
[9] C. Stambaugh and H. B. Chan, Phys. Rev. B **73**, 172302 (2006).
[10] J. S. Aldridge and A. N. Cleland, Phys. Rev. Lett. **94**, 156403 (2005).
[11] R. L. Badzey, G. Zolfagharkhani, A. Gaidarzhy, and P. Mohanty, Appl. Phys. Lett. **86**, 023106 (2005).
[12] B. J. Keay, S. J. Allen, Jr., J. Galán, J. P. Kaminski, K. L. Campman, A. C. Gossard, U. Bhattacharya, and M. J. W. Rodwell, Phys. Rev. Lett. **75**, 4098 (1995).
[13] H. A. Kramers, Physica (Amsterdam) **7**, 284 (1940).
[14] M. I. Dykman and M. A. Krivoglaz, Physica A **104**, 408 (1980).
[15] V. I. Mel'nikov and S. V. Meshkov, J. Chem. Phys. **85**, 1018 (1986).
[16] M. I. Dykman, I. B. Schwartz, and M. Shapiro, Phys. Rev. E **72**, 021102 (2005).
[17] R. Graham and T. Tél, Phys. Rev. A **31**, 1109 (1985).
[18] R. S. Maier and D. L. Stein, SIAM J. Appl. Math. **57**, 752 (1997).
[19] D. Ryvkine, M. I. Dykman, and B. Golding, Phys. Rev. E **69**, 061102 (2004).
[20] J. Lehmann, P. Reimann, and P. Hänggi, Phys. Rev. E **62**, 6282 (2000).
[21] M. I. Dykman, D. G. Luchinsky, R. Mannella, P. V. E. McClintock, N. D. Stein, and N. G. Stocks, Phys. Rev. E **49**, 1198 (1994).
[22] L. Gammaitoni, P. Hänggi, P. Jung, and F. Marchesoni, Rev. Mod. Phys. **70**, 223 (1998).
[23] H. S. Wio, P. Colet, M. S. Miguel, L. Pesquera, and M. A. Rodriguez, Phys. Rev. A **40**, 7312 (1989).
[24] S. J. B. Einchcomb and A. J. McKane, Phys. Rev. E **51**, 2974 (1995).
[25] P. Hänggi, J. Stat. Phys. **42**, 105 (1986).
[26] O. A. Tretiakov, T. Gramespacher, and K. A. Matveev, Phys. Rev. B **67**, 073303 (2003); O. A. Tretiakov and K. A. Matveev, Phys. Rev. B **71**, 165326 (2005).
[27] B. Abdo, E. Segev, O. Shtempluck, and E. Buks, IEEE Trans. Appl. Supercond. **16**, 1976 (2006).
[28] B. Abdo, E. Segev, O. Shtempluck, and E. Buks, Phys. Rev. B **73**, 134513 (2006).
[29] B. Abdo, E. Segev, O. Shtempluck, and E. Buks, Appl. Phys. Lett. **88**, 022508 (2006).
[30] B. Abdo, E. Segev, O. Shtempluck, and E. Buks, cond-mat/0606555.
[31] E. Segev, B. Abdo, O. Shtempluck, and E. Buks, cond-mat/0607259.
[32] E. Segev, B. Abdo, O. Shtempluck, and E. Buks, J. Phys.: Condens. Matter **19**, 096206 (2007).
[33] E. Segev, B. Abdo, O. Shtempluck, and E. Buks, Phys. Lett. A (to be published).
[34] B. Yurke and E. Buks, J. Lightwave Technol. **24**, 5054 (2006).
[35] C. W. Gardiner and M. J. Collett, Phys. Rev. A **31**, 3761 (1985).
[36] A. V. I. Gurevich and R. G. Mints, Rev. Mod. Phys. **59**, 941 (1987).
[37] B. Abdo, E. Segev, O. Shtempluck, and E. Buks, IEEE Trans. Appl. Supercond. (in press); cond-mat/0501236.
[38] M. W. Johnson, A. M. Herr, and A. M. Kadin, J. Appl. Phys. **79**, 7069 (1996).
[39] A. M. Kadin and M. W. Johnson, Appl. Phys. Lett. **69**, 3938 (1996).
[40] K. Weiser, U. Strom, S. A. Wolf, and D. U. Gubser, J. Appl. Phys. **52**, 4888 (1981).